Investigation of Intramolecular Hydrogen−Deuterium Exchange in the Time-of-Flight Secondary-Ion Mass Spectra of Polystyrene

Lucinda R. Hittle, Andrew Proctor, and David M. Hercules*

Department of Chemistry, University of Pittsburgh, Pittsburgh, Pennsylvania 15260

Received December 19, 1994; Revised Manuscript Received April 4, 1995[⊗]

ABSTRACT: Partially deuterated polystyrenes (PS-d_3 and PS-d_5) were examined using TOF-SIMS and regression analysis. Intramolecular H/D exchange was observed for both small fragment ions ($C_6H_7^+$, *etc.*) and for main chain fragments in the mass range from 500 to 3000 Da. Depending on the type of fragment, either one or two exchanges occur. Facile H/D mixing between the polymer backbone and the phenyl ring must occur during formation of all types of fragments. Comparison of the results from regression analysis showed that for PS-d_3 *hydrogen* abstraction by the chain backbone occurred much more readily than the corresponding *deuterium* abstraction for PS-d_5.

Introduction

Recently, an investigation of H/D mixing during polystyrene ion formation, induced by kiloelectronvolt Ar ions, was conducted in our laboratory using time-of-flight secondary ion mass spectrometry (TOF-SIMS).[1] In that study, perdeuterio- (PS-d_8) and perhydropolystyrene mixtures were analyzed. Based on the results of several data analysis techniques, including regression analysis and principal component analysis, no significant amount of H/D exchange was observed for these mixtures. Thus, we concluded that hydrogen abstraction during SIMS ion formation must occur mainly via *intra*molecular rather than *inter*molecular mechanisms.

Several types of mass spectrometry, including fast atom bombardment (FAB),[2,3] electrospray,[4,5] and SIMS[6,7] have utilized H/D exchange to determine the number of labile hydrogens within an analyte molecule. The labile hydrogens were typically those of hydroxyl or amide groups which underwent H/D exchange with the matrix or solvent during ion formation. Although these studies have provided information about mechanisms of intermolecular exchange between the analyte molecule and the matrix, *intra*molecular H/D exchange has not been investigated as extensively. However, intramolecular H/D exchange was observed in a SIMS study of partially deuterated polystyrene by Chilkoti *et al.*[8] They found that small fragment ions (1−200 Da) of PS-d_3 and -d_5 showed significant amounts of H/D exchange during formation of such species as tropylium ions.[8] Facile H/D migration occurred between the polymer backbone and the phenyl group at some point during ion formation. Additionally, a SIMS investivation of intramolecular H/D exchange in random copolymers of styrene and deuteriostyrene was reported by Affrossman *et al.*[9] A significant amount of H/D mixing during tropylium ion formation was also observed for these random copolymers.

TOF-SIMS has previously been used to study fragmentation mechanisms for several types of polystyrene.[10] Fragmentation of the polymer backbone was explained by limited chain fragmentation, consistent with mechanisms proposed for other methods. The spectra consisted of a series of repeating patterns, the spacing of which corresponded to the mass of the repeat unit. When the fine structure of polystyrene main chain fragment clusters was examined, typical fragment ions were found to contain either zero, one, or two double bonds. The abundance of these three types of species within a given cluster indicated that mechanisms other than the proposed "diradical intermediate" model were involved in ion formation.

The purpose of the present study is to use TOF-SIMS to determine the extent and mechanisms of intramolecular H/D exchange during formation of high molecular weight (500−3000 Da) main chain fragments for partially deuterated polystyrene. Elucidation of the processes governing hydrogen transfer and abstraction should allow a greater understanding of SIMS ion formation mechanisms. In addition, the effect of polymer molecular weight on the observed fragmentation patterns will be addressed.

Experimental Section

TOF-SIMS. Instrumentation. The instrument used in these studies was a time-of-flight secondary-ion mass spectrometer, TOF-SIMS III, designed and manufactured by Ion-Tof GmbH, Münster, Germany. This instrument was designed for analysis of biomolecules on the pico- and femtomole level, but it has also been used for analysis of semiconductors and polymers.[11] In essence the instrument consists of two main components: (1) a pulsed Ar^+ primary ion source and (2) a TOF reflectron analyzer/detector system. The TOF-SIMS has been described in more complete detail elsewhere.[12,13] The primary ion gun consists of a standard electron impact argon ion source combined with a pulsed 90° deflector for beam chopping and primary ion mass separation, followed by an axial buncher for pulse compression. The resultant mass-separated primary ion bunches have a typical pulse length of about 1 ns and a variable spot diameter between 5 and 50 μm.

Secondary ions generated by a primary ion pulse on the target surface are extracted and accelerated to an energy of 3 keV. In the following 2 m flight path, an Einzel lens and reflectron optics are integrated for focusing the secondary ion beam and for energy compensation, respectively. To achieve high detection efficiency, in particular for molecular ions in the high-mass range, the ions are postaccelerated to 10 keV, where they are then detected by a channel plate−scintillator−photomultiplier combination.

The data collection system consists of a time-to-digital converter, a fast buffer memory, and an accumulating memory board. The spectra are accumulated in the single ion counting mode with a maximum of 256 stops/pulse, a time resolution of 1.25 ns/channel, and a total time range of 320 μs. The cycle time was set at 200 μs, allowing investigation of ions from 1 to 4000 Da. The base pressure of the main chamber of the instrument was typically 3×10^{-8} Pa, and the operating pressure was approximately 1×10^{-6} Pa, with a pressure of 4×10^{-4} Pa in the primary ion source. During the analysis the

[⊗] Abstract published in *Advance ACS Abstracts,* August 1, 1995.

0024-9297/95/2228-6238$09.00/0

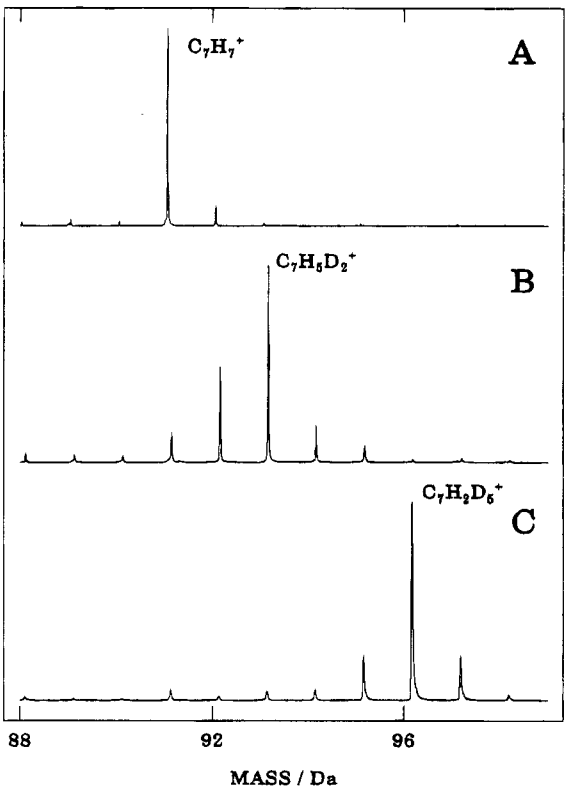

Figure 1. Low-mass spectra from 88 to 98 Da for (A) HPS, (B) PS-d_3, (C) PS-d_5.

target was bombarded by a 10 keV Ar^+ beam with an average pulsed primary ion current of 0.5−1.0 pA for a total collection time of 200 s. The total primary ion dose was less than 10^{13} ions/cm^2 (static SIMS). Typical resolution ($m/\Delta m$) was 8000 at m/z = 1000.

Sample Preparation and Data Analysis. Perhydropolystyrene (HPS) samples of varied molecular weights were obtained from Scientific Polymer Products (Ontario, NY). Polystyrene deuterated only along the chain backbone (PS-d_3) was obtained from Polymer Laboratories (Amherst, MA) and had an M_n of 7400 and an M_w of 7700. Ring-deuterated polystyrene (PS-d_5) was obtained from Cambridge Isotope Laboratories (Woburn, MA), and had an approximate molecular weight of 70 000. The extent of deuteration (>98%) for the PS-d_3 and PS-d_5 samples was verified by ^{1}H and ^{13}C NMR analysis. Samples were prepared for SIMS analysis by dissolving the polymer in toluene. Typical solution concentrations were 10^{-3} M with respect to the repeat unit. Sample volumes of 1−5 μL were deposited on a silver target with an area of about 12 mm^2. The silver had been etched in nitric acid (20 vol %) and rinsed with deionized water and methanol.

All of the data analysis procedures were performed using in-house-generated software (GOOGLY by A.P.) written for an IBM PC compatible under MS DOS.

Results and Discussion

1. Low-Mass Region (<500 Da). One of the most interesting features of the TOF-SIMS spectra of partially deuterated polystyrene concerns the tropylium ion in the low-mass region. Figure 1 shows the mass region from 88 to 99 Da for HPS, polystyrene-α,β,β-d_3 (PS-d_3), and polystyrene-ring-d_5 (PS-d_5). An intense peak at 91 Da is observed for HPS for the $C_7H_7^+$ ion. The corresponding peak at 93 Da ($C_7H_5D_2^+$) was observed for PS-d_3 along with a relatively intense peak at 92 Da for the species $C_7H_6D^+$. Formation of the tropylium ion should involve cleavage of a benzyl ion from the polymer chain, along with abstraction of a deuterium from the chain backbone. Expansion of the phenyl ring to a seven-membered aromatic species will also occur in this mechanism. Thus, the $C_7H_5D_2^+$ species has the highest probability of forming for PS-d_3. Formation of the $C_7H_6D^+$ species must arise either from hydrogen transfer by one of the hydrogen-containing end groups (C_4H_9− or H−) or from neighboring phenyl rings.

The spectrum for PS-d_5, shown in Figure 1C, contains an intense peak at 96 Da corresponding to $C_7D_5H_2^+$. Weaker peaks at 95 and 97 Da for the $C_7D_4H_3^+$ and $C_7D_6H^+$ species, respectively, are also observed. The $C_7D_6H^+$ species produced by deuterium abstraction from a neighboring phenyl group is proportionately much less intense than the species produced by phenyl group hydrogen abstraction for PS-d_3 ($C_7H_6D^+$). Preferential hydrogen, rather than deuterium, abstraction may be explained by a kinetic isotope effect.[14] Intramolecular H/D exchange was also observed for other PS-d_3 and -d_5 fragments in the low-mass region. For example, fairly intense $C_6H_4D^+$ and $C_6H_3D_2^+$ ions at 78 and 79 Da were observed in addition to the $C_6H_5^+$ ion at 77 Da for PS-d_3, indicating that H/D scrambling had occurred involving the phenyl ring. Surprisingly, energetically unfavorable hydrogen abstraction from the phenyl ring occurs during the formation of small fragment ions, and to a greater extent than the corresponding deuterium abstraction process seen for PS-d_5.

In general, the low-mass spectra were very similar to those obtained by Chilkoti *et al.*; however, an intense peak was not observed at 92 Da in their spectrum of PS-d_3.[8] This difference in intensities could be caused by two possible experimental factors: (1) sample preparation or (2) ion doses. Their quadrupole SIMS spectra were obtained for thick polymer samples spin coated on Si wafers, whereas our sample preparation involves casting a thin film on an etched silver surface (*ca.* 0.5 monolayer coverage[15]). Abstraction of a hydrogen from an end group may be much easier at lower coverages, because of less polymer entanglement. When the concentration of the solution cast on silver was increased to produce multilayer coverage, no changes in the relative intensities of the peaks at 92, 93, and 94 Da were observed. Thus, the differences in the spectra from the two studies are not simply related to sample film thickness, but may be caused by solvent effects on the surface conformation/orientation. It should also be mentioned that the polystyrene samples analyzed in these two studies were the same molecular weight and composition.

The other possible reason for dissimilarity between the two spectra may be different ion doses. Cooks and co-workers found that the extent of intermolecular H/D exchange between the analyte and a ND_4Cl matrix is dependent upon primary ion dose when operating under static SIMS conditions.[6] However, in this study when the dose was varied between 1×10^{11} and 8×10^{13} Ar^+ ions/cm^2 (above the static limit) for the PS-d_3 sample, the relative intensities of the peaks at 92, 93, and 94 Da varied by less than 2%. Analysis of the three polystyrene samples using a quadrupole SIMS instrument yielded spectra essentially identical to those obtained by Chilkoti *et al.* Another possible reason for the differences in the spectra might be the detection efficiencies of quadrupole versus time-of-flight analyzers.

Tandem mass spectrometric studies of polystyrene by Leggett *et al.*[16] have shown that daughter ion spectra of fragments corresponding to one or more monomer units do not contain a peak at 91 Da for the tropylium

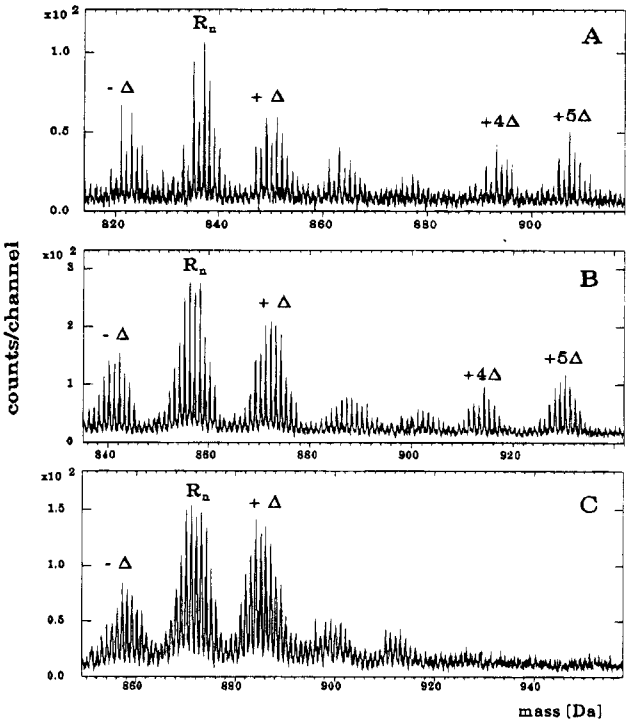

Figure 2. Typical fragment pattern for (A) HPS molecular weight 7000, (B) PS-d_3 molecular weight 7000; (C) PS-d_5 molecular weight 70 000.

ion. Leggett *et al.* believe that the tropylium ion is formed by a mechanism different from free radical chain cleavage; perhaps it is somehow directly ejected from the sample surface, rather than produced by fragmentation of a larger polymer ion. Since the primary ion dose and sample thickness have no effect on the extent of intramolecular H/D exchange for the tropylium ion, the ion formation mechanism must be independent of surface damage and geometry.

2. High-Mass Region (500–3000 Da). The following terminology will be used to describe the TOF-SIMS spectra: *fragment* will refer to a segment from a polymer chain; *cluster* will refer to a group of peaks for a mass range of *ca.* 10 Da corresponding to a particular ion; and *pattern* will refer to a repeating sequence of clusters in the TOF-SIMS spectrum. The term Δ will refer to the spacing between clusters (CH_n groups approximately 12–15 Da), and R_n will refer to a fragment containing an integral number of repeat units. The terms R_n, $R_n + \Delta$, $R_n - \Delta$, *etc.* are used to generalize the structural formulas of main chain fragments within a pattern. It is understood that these types of fragments may result from different oligomers. A more extensive description of this nomenclature is given in ref 9.

Details of a typical fragmentation pattern for HPS are shown in Figure 2A. Clusters approximately 14 mass units apart can be seen for the fragments R_n, $R_n - \Delta$, $R_n + \Delta$, $R_n + 2\Delta$, $R_n + 3\Delta$, $R_n + 4\Delta$, and $R_n + 5\Delta$. The fragmentation mechanisms for these species have previously been described in great detail,[10] with the exception of the $R_n + 4\Delta$ and $R_n + 5\Delta$ fragments, which result from single cleavage of the polymer chain to produce ions containing the *tert*-butyl terminal group (R_n—C_4H_9 or CH_2=R_n—C_4H_9). The fragmentation pattern of much higher molecular mass polystyrene (75 000 Da) did not contain peaks corresponding to $R_n + 4\Delta$ and $R_n + 5\Delta$ fragments.[10] In order to determine if these $R_n + 4\Delta$ and $R_n + 5\Delta$ clusters were related to polymer molecular weight or were simply anomalies for a single sample, a

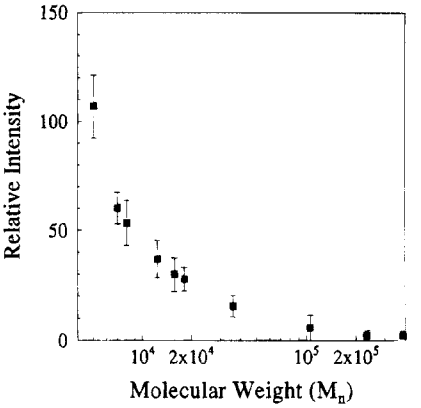

Figure 3. Relative intensity of $R_n + 5\Delta$ fragment cluster vs sample molecular weight (M_n) for HPS. Relative intensities were calculated by ratioing the cluster intensity to the R_n peak intensity, which was set at 100%. Error bars represent one standard deviation of the mean.

Table 1. Relative Cluster Intensity as a Function of Molecular Weight for HPS[a]

mol wt	+4Δ	+5Δ	−Δ	+Δ
5 000	86 ± 15	107 ± 14	34 ± 5.2	27.6 ± 2.8
7 000	43 ± 7	60 ± 7	52 ± 12	85.3 ± 9.7
8 000	41 ± 6	54 ± 10	50 ± 4	77 ± 2
12 400	30 ± 6	37 ± 8	23 ± 2	45 ± 3
15 800	22 ± 7	30 ± 7	37 ± 6	78 ± 13
18 100	21 ± 5	28 ± 5	52 ± 5	92 ± 7
36 000	11 ± 4	13 ± 6	39 ± 14	100 ± 9
106 000	6 ± 5	6 ± 5	48 ± 5	78 ± 6
233 000	5 ± 6	2 ± 2	39 ± 7	97 ± 9
387 000	7 ± 6	2 ± 1	47 ± 11	106 ± 12

[a] Values are means of 4–6 measurements ± standard deviation.

series of polystyrene samples having different molecular weights were analyzed. The relative intensities of the terminal group fragment ion series $R_n + 5\Delta$ for HPS were calculated as the ratio of the $R_n + 5\Delta$ intensity to the intensity of the R_n ions (expressed as percent) and are shown in Figure 3. Results were obtained by averaging the values for five patterns within a given spectrum for each molecular weight. The relative intensity of the $R_n + 5\Delta$ fragment ion decreases in an exponential fashion with increasing molecular weight. Similar results were observed for the $R_n + 4\Delta$ fragment ion series. The relative intensities of the four major fragment clusters are listed in Table 1 for the range of sample molecular weights studied. The relative intensities were calculated by ratioing the cluster intensity to the R_n peak intensity, which was set at 100%. Surprisingly, these fragment ions containing a terminal group are observed in the spectra of relatively high molecular weight polystyrenes. TOF-SIMS spectra of the majority of polymers with molecular masses greater than *ca.* 5000 Da do not generally show peaks corresponding to a main chain fragment plus a terminal group. For example, analysis of diacrylate- and distearate-terminated poly(ethylene glycol)s with molecular weights from 4000 to 6000 did not show additional fragment clusters, although the individual species within the main fragment clusters were different.[17]

Figure 4 shows the relative intensity of the $R_n - \Delta$ fragment clusters as a function of sample molecular weight. These fragments resulting from a two-step chain cleavage mechanism showed more or less random fluctuations in the relative cluster intensity when the sample molecular weight was varied. The $R_n + 4\Delta$ and $R_n + 5\Delta$ fragments arise from single cleavage of the polymer chain, which is most important for relatively

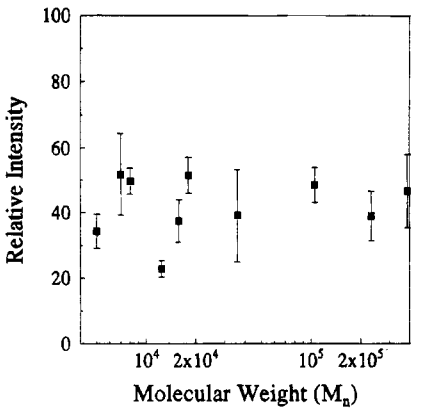

Figure 4. Relative intensity of $R_n - \Delta$ fragment cluster vs sample molecular weight (M_n) for HPS. Relative intensities were calculated by ratioing the cluster intensity to the R_n peak intensity, which was set at 100%. Error bars represent one standard deviation of the mean.

low molecular weight polymers. As the polymer molecular weight increases, the polymer chain length becomes significantly larger than the "action area" (40–60 Å) of the primary ion beam, and the number of terminal groups becomes relatively small with respect to the number of repeat units in the polymer chain. At this point, the dominant fragmentation process involves two separate cleavages of the polymer chain rather than single cleavage or desorption of the intact oligomer. This effect has also been observed in the fragmentation of polybutadienes.[18] Fragmentation mechanisms following the diradical cleavage model are essentially independent of molecular weight.

Typical fragment patterns for PS-d_3 and -d_5 in the high-mass range are shown in Figure 2B,C. When compared with the HPS spectrum in Figure 2A, it can be seen that the PS-d_3 and PS-d_5 spectra contain similar patterns of fragment clusters (R_n, $R_n + \Delta$, *etc.*) and that the fine structure of the individual clusters indicates more species than those of the HPS. In order to determine exactly what species are contained within the individual clusters, linear least squares regression analysis (LLSRA) was carried out. Unlike the pattern matching algorithms which have been used to study H/D exchange in FAB mass spectra,[3] LLSRA offers the advantage of providing a quantitative estimate of the contribution of individual components to the overall peak envelope. Prior to data analysis, the fragment clusters from five patterns within a spectrum were added and smoothed using a Reinsch-spline function.[19] Difficulties from slight changes in experimental peak shapes were circumvented by regenerating the experimental peaks with a Gaussian shape. The fragment clusters were then fitted using a series of theoretical isotopic patterns of the same basic peak shape. An increasing number of components was used to fit the data, and the residual was examined after each additional component. When the residual was random, it was assumed that the correct number of species had been used. F-testing was also used to verify the validity of the number of components. All of the concentrations obtained by LLSRA are listed as the average analysis of six to eight spectra for each sample, along with the resultant standard deviation of the mean.

Before the extent of intramolecular H/D exchange could be determined, the number of unsaturations within all of the fragment clusters for HPS were calculated by curve fitting. LLSRA of substituted polystyrenes has previously been conducted to determine the number of unsaturations within R_n clusters and showed species corresponding to 0, 1, and 2 degrees of unsaturation.[10] Results for R_n, $R_n + \Delta$, $R_n - \Delta$, $R_n + 4\Delta$, and $R_n + 5\Delta$ fragment clusters of HPS are listed in Table 2. The $R_n + 4\Delta$ and $R_n + 5\Delta$ fragments can only be formed by single cleavage of the polymer backbone at the α or β C–C bond to produce either a secondary ($+4\Delta$) or primary ($+5\Delta$) carbon radical, rather than by two separate cleavages. Thus, the only possibilities are either zero or one double bond. Species corresponding to two degrees of unsaturation were not observed experimentally within the $R_n + 4\Delta$ and $R_n + 5\Delta$ fragment clusters. Statistically, zero or one degree of unsaturation should occur in approximately a 50:50 ratio for both $R_n + 4\Delta$ and $R_n + 5\Delta$ clusters. The actual ratios for 0:1 degree of unsaturation were 47:53 for $R_n + 4\Delta$ (1:1) and 34:66 for $R_n + 5\Delta$ (1:2). The difference in these ratios for the two fragments may be explained by the nature of the radical species. The secondary radical present for the $R_n + 4\Delta$ fragment may abstract a hydrogen or form a double bond with equal probability, whereas the primary radical for $R_n + 5\Delta$ prefers to form a double bond.

Table 2. Linear Least Squares Regression Analysis of HPS Fragment Clusters[a]

	no. of unsaturations		
cluster	0	1	2
R_n	25 ± 9	55.4 ± 7.4	20 ± 8
$R_n + \Delta$	18 ± 6	27.6 ± 18.5	54 ± 17
$R_n - \Delta$	26 ± 14	58.7 ± 14.3	15 ± 5
$R_n + 4\Delta$	47 ± 9	53.0 ± 9.4	
$R_n + 5\Delta$	35 ± 5	65 ± 5	

[a] Values are means of 4–6 measurements ± standard deviation.

The values for the R_n cluster were also close to the theoretical ratio of 1:2:1,[10] with values of 25:55:20 for 0:1:2 degrees of unsaturation. Unfortunately, the other two fragment clusters do not follow the simple statistical model proposed for the diradical intermediate in which the intensity ratio for 0:1:2 degrees of unsaturation should be 1:2:1. The 0:1:2 unsaturation ratio for $R_n + \Delta$ is 18:28:54 (~2:3:6) and for $R_n - \Delta$ is 26:59:15 (~2:4:1). It should be emphasized that these numbers are merely approximations, since there is considerable variability in the relative abundances of these components. This deviation from the simple statistical model may be explained by the nature of the radical fragment. Two separate chain scissions will generate at the chain ends two primary radicals for $R_n + \Delta$ and two secondary radicals for the $R_n - \Delta$ fragment. Based on the experimentally observed unsaturation ratios for the $R_n + \Delta$ and $R_n - \Delta$ fragments as well as those for the $R_n + 4\Delta$ and $R_n + 5\Delta$ fragments, formation of a double bond appears to be more favored for a primary radical, and a secondary radical may either abstract a hydrogen or form a double bond, with equal probability. Since the presence of a cyclic intermediate during polystyrene fragmentation has already been shown,[10] the formation of cyclic polystyrene ions should also be considered and may account for differences between the experimental and theoretical unsaturation ratios.

After examination of the number of unsaturations in the HPS fragment cluster, LLSRA was conducted to determine the number of H/D exchanges for PS-d_3 and PS-d_5. The fragment clusters were fitted with theoretical isotopic distributions corresponding to 0, 1, or 2 H/D exchanges and 0, 1, or 2 unsaturations. A maximum of nine possible components could be contained within

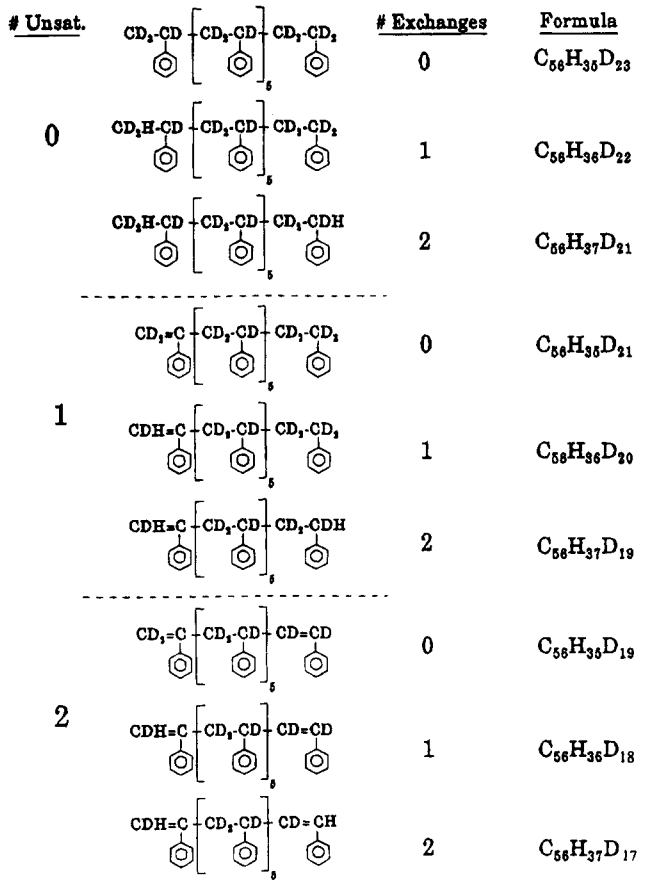

Figure 5. Possible structures resulting from H/D exchange for the PS-d_3 R_n fragment.

a given fragment cluster; possible structures for the R_n cluster are shown in Figure 5. Once again, since the $R_n + 4\Delta$ and $R_n + 5\Delta$ clusters arise from single (rather than double) scission, only patterns with zero or one unsaturations and 0 or 1 H/D exhanges were considered.

Typical results from LLSRA are shown in Figure 6 for a PS-d_5 $R_n + \Delta$ cluster fitted with six different components. The experimental data are shown in the figure as individual points, with the overall fit overlaid on top of the points. The individual components used in LLSRA are shown as curves underneath the overall envelope (a–f in the figure). The contributions of the individual components to the overall envelope are indicated by the relative intensities shown. In general, good agreement between the actual data and the overall fit was observed. LLSRA results for the PS-d_3 fragment clusters of interest are listed in Table 3. Each type of fragment cluster showed a significant contribution from at least one component resulting from H/D exchange. Thus, LLSRA provides clear evidence of intramolecular H/D exchange. H/D exchange by either an intermolecular process or from hydrogen contaminants on the silver substrate can be disregarded since these processes did not occur significantly for perdeuteriopolystyrene.[1] Each of the five types of fragment clusters showed at least one, if not two exchanged hydrogens. In general, the component of greatest intensity corresponds to one unsaturation with either zero or one exchange. Another observation of note is that the extent of double bond formation changes when deuterium is added to the polymer backbone, which may, once again, be caused by a kinetic isotope effect. For example, the $R_n - \Delta$ cluster had a ratio of 0:1:2 unsaturations of 26:59:15 in HPS but in PS-d_3 the ratio is 43:47:10. For the R_n and

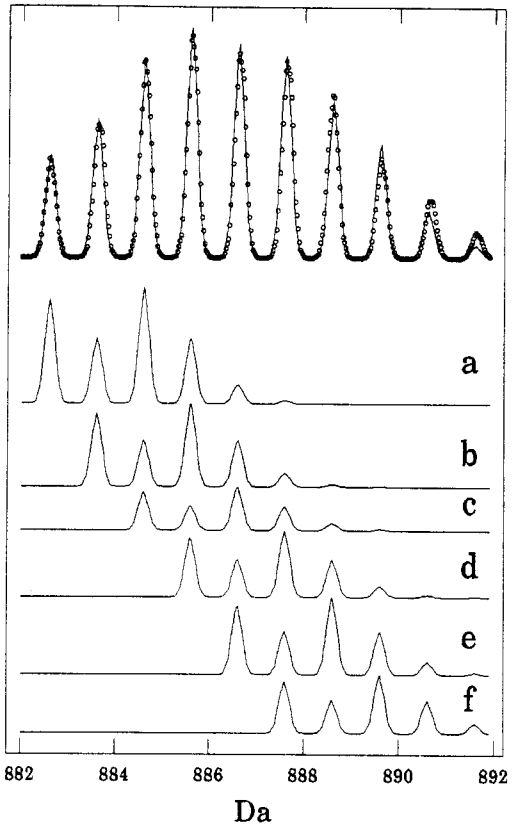

Figure 6. Typical results for linear least squares regression analysis of PS-d_5, $R_n + \Delta$ cluster containing six components. Individual components are shown as curves underneath the overall fit. (a) 2 unsat, 0 exchanges; (b) 1 unsat, 1 exchange; (c) 1 unsat, 0 exchanges or 2 unsat, 2 exchanges; (d) 1 unsat, 1 exchange; (e) 0 unsat, 0 exchanges or 1 unsat, 2 exchanges; (f) 0 unsat, 1 exchange.

Table 3. Linear Least Squares Regression Analysis of PS-d_3 Clusters[a]

no. of H/D exchanges	cluster	no. of unsaturations 0	1	2
0	R_n	– – –[b]	26 ± 3	17 ± 2
	$R_n + \Delta$	– – –	21 ± 5	23 ± 2
	$R_n - \Delta$	2 ± 2	26 ± 2	10 ± 1
1	R_n	– – –	28 ± 4	– – –
	$R_n + \Delta$	– – –	27 ± 2	– – –
	$R_n - \Delta$	29 ± 2	21 ± 1	– – –
2	R_n	19 ± 11	9 ± 5	– – –
	$R_n + \Delta$	15 ± 3	14 ± 4	– – –
	$R_n - \Delta$	11 ± 5	– – –	– – –
0	$R_n + 4\Delta$	22 ± 10	23 ± 6	
	$R_n + 5\Delta$	10 ± 6	37 ± 6	
1	$R_n + 4\Delta$	34 ± 7	21 ± 3	
	$R_n + 5\Delta$	32 ± 4	20 ± 5	

[a] Values are means of 4–6 measurements ± standard deviation. [b] – = species not observed.

$R_n + \Delta$ clusters, a change in the unsaturation from 1:2:1 to 1:3:1 (actual values 19:64:17 for R_n and 15:62:23 for $R_n + \Delta$) was observed, suggesting preferential formation of a singly unsaturated species for these fragments. The relative proportions of the number of unsaturations for the R_n, $R_n + 4\Delta$, and $R_n + 5\Delta$ clusters for PS-d_3 are similar to those for HPS. The extent of H/D exchanges is also similar for the $R_n + 4\Delta$ and $R_n + 5\Delta$ clusters, indicating the hydrogen abstraction mechanism is unaffected by the deuterium isotope effect for the single radical species.

The results for LLSRA of the PS-d_5 sample are shown in Table 4. Unfortunately, two sets of the theoretical

Table 4. Linear Least Squares Regression Analysis of PS-d_5 Fragment Clusters[a]

no. of H/D exchanges	cluster	no. of unsaturations 0	1	2
0	R_n	13. 0 ± 2	15 ± 2	28 ± 6
	$R_n + \Delta$	18 ± 1.7	5 ± 3	36 ± 5
	$R_n - \Delta$	16 ± 6	13 ± 9	24 ± 3
1	R_n	9 ± 5	9 ± 6	27 ± 6
	$R_n + \Delta$	7 ± 3	8 ± 4	26 ± 4
	$R_n - \Delta$	5 ± 4	21 ± 2	20 ± 2
2	R_n	– – –	*c*	*d*
	$R_n + \Delta$	– – –	*c*	*d*
	$R_n - \Delta$	– – –	*c*	*d*

[a] Values are means of 4–6 measurements ± standard deviation. [b] – – = species not observed. [c] Pattern isobaric with that of zero unsaturations, no exchanges. [d] Pattern isobaric with that of one unsaturation, no exchanges.

patterns for PS-d_5 were identical, making it impossible to differentiate between them. For example, a fragment containing one unsaturation and no H/D exchanges and a fragment containing two unsaturations and two H/D exchanges have the same mass (isobars). Additionally, $R_n + 4\Delta$ and $R_n + 5\Delta$ fragments were not observed in the PS-d_5 spectrum due to its molecular mass (70 kDa). Although the isobaric patterns make quantitative interpretation impossible, H/D exchange was also observed in PS-d_5 fragments. All three types of fragments (R_n, $R_n + \Delta$, and $R_n - \Delta$) contained a component of significantly intensity for two unsaturations and one H/D exchange. However, the components for zero and one unsaturation, with one exchange, are generally less intense. Similar to the isotope effect observed for the hydrogen abstraction of the tropylium ion, H/D mixing seems less extensive for PS-d_5 when compared with PS-d_3.

Even though hydrogens can be readily abstracted from the end groups, this mechanism cannot account for the propensity of H/D exchange observed for all types of fragments and both types of deuterated polystyrene. Randomization of the hydrogens and deuteriums between the polymer backbone and the phenyl ring must readily occur. Two possible explanations for this behavior may be proposed. A hydrogen or deuterium may be abstracted directly from a phenyl ring by attack of a radical chain end produced by initial chain cleavage. The second possibility is that the phenyl ring expands immediately after chain cleavage, which randomizes the hydrogens and deuteriums. A fragment ion is then produced by the decomposition of this cyclic seven- to ten-membered species. Due to the amount of energy (kiloelectronvolt) imparted to the polymer molecule by the collisional cascade of the primary ion beam, the second possibility seems more likely, but even energetically unfavorable processes may occur during SIMS ion formation. Although the exact mechanism(s) of hydrogen abstraction and transfer cannot be pinpointed, it is clear that these reactions do not occur solely along the polymer backbone. Thus, the effect of chain substituents, such as phenyl or methyl groups, should also be considered when describing general polymer fragmentation mechanisms.

Conclusions

The fragmentation patterns observed in the spectra of polystyrenes with a range of molecular weights were found to contain clusters corresponding to single chain cleavage for low to medium molecular mass polymers (<20 000 Da). Single cleavage of the polymer chain occurs only if the chain length of the polymer is not appreciably larger than the area of the substrate affected by the impact of the primary ion. The mechanisms of hydrogen abstraction and double bond formation were found to be dependent on the type of radical (primary versus secondary) and the number of chain scissions which produce the ion (single versus diradical).

Partially deuterated polystyrenes (PS-d_3 and PS-d_5) were examined using TOF-SIMS and regression analysis. Intramolecular H/D exchange was observed for both small fragment ions ($C_7H_7^+$, *etc.*) and for main chain fragments in the mass range from 500 to 3000 Da. Depending on the type of fragment, either one or two exchanges have been shown to occur. Facile H/D mixing between the polymer backbone and the phenyl ring must occur during formation of all types of fragments. Comparison of the results from regression analysis for PS-d_3 to those for PS-d_5 showed that for PS-d_3 abstraction of hydrogen by the chain backbone occurred much more readily than deuterium abstraction for PS-d_5.

Acknowledgment. This work was supported by the National Science Foundation (Grants CHE-90221335 and INT-9244276). L.R.H. would like to thank Dow Chemical Corp. for a graduate fellowship. The authors would also like to thank Paul Danis for donating the polystyrene-d_3 sample, Buddy Ratner for donating the polystyrene-d_5 sample, Fu-Tyan Lin for conducting the NMR analysis, and Ed Goralski for conducting the comparative quadrupole SIMS analysis.

References and Notes

(1) Hittle, L. R.; Proctor, A.; Hercules, D. M. *Anal. Chem.* **1994**, *66* (1), 108–114.
(2) Guarini, A.; Guglielmetti, G.; Andriollo, N.; Vincenti, M. *Anal. Chem.* **1992**, *64*, 204–210.
(3) Verma, S.; Pomerantz, S. C.; Sethi, S. K.; McCloskey, J. A. *Anal. Chem.* **1986**, *58*, 2898–2902.
(4) Chi, H. T.; Baker, J. T. *Org. Mass Spectrom.* **1993**, *28*, 12–17.
(5) Siegel, M. M. *Anal. Chem.* **1988**, *60*, 2090–2095.
(6) Hand, O. W.; Ranasinghe, A.; Cooks, R. G. *Org. Mass Spectrom.* **1993**, *28*, 176–184.
(7) Bentz, B. A.; Gale, P. J. *Int. J. Mass Spectrom. Ion Processes* **1987**, *78*, 115–130.
(8) Chilkoti, A.; Castner, D. G.; Ratner, B. D. *Appl. Spectrosc.* **1991**, *45* (2), 209–217.
(9) Affrossman, S.; Hartshorne, M.; Jerome, R.; Munro, H.; Pethrick, R. A.; Petitjean, S.; Rei Vilar, M. *Macromolecules* **1993**, *26*, 5400–5405.
(10) Chiarelli, M. P.; Proctor, A.; Bletsos, I. V.; Hercules, D. M.; Feld, H.; Leute, A.; Benninghoven, A. *Macromolecules* **1992**, *25*, 6970–6976.
(11) Niehuis, E. In *Secondary Ion Mass Spectroscopy (SIMS VII)*; Benninghoven, A., Ed.; Wiley-Interscience: Chichester, U.K., 1989; pp 299–304.
(12) Niehuis, E.; Heller, T.; Feld, H.; Benninghoven, A. *J. Vac. Sci. Technol. A* **1987**, *5* (4), 1243–1246.
(13) Niehuis, E.; van Veltzen, P. N. T.; Lub, J.; Heller, T.; Benninghoven, A. *Surf. Interface Anal.* **1989**, *14*, 135–142.
(14) Loudon, G. M. *Organic Chemistry*; Addison-Wesley; Reading, MA; pp 162–164.
(15) Muddiman, D. M.; Brockman, A. H.; Proctor, A.; Houalla, M.; Hercules, D. M. Submitted to *J. Phys. Chem.*
(16) Leggett, G. J.; Vickerman, J. C.; Briggs, D.; Hearn, M. J. *J. Chem. Soc., Faraday Trans.* **1992**, *88* (3), 297–309.
(17) Hittle, L. R.; Altland, D. E.; Proctor, A.; Hercules, D. M. *Anal. Chem.* **1994**, *66* (14), 2302–2312.
(18) Hittle, L. R.; Hercules, D. M. *Surf. Interface Anal.* **1994**, *21*, 217–225.
(19) Proctor, A.; Fay, M. J.; Hoffmann, D. P.; Hercules, D. M. *Appl. Spectrosc.* **1990**, *44* (6), 1052–1056.

MA9463674